

ARTICLES

Quantum phase transitions of the one-dimensional Peierls-Hubbard model with next-nearest-neighbor hopping integrals

Hiromi Otsuka

Department of Physics, Tokyo Metropolitan University, Tokyo 192-0397, Japan

(Received 4 February 1998)

We investigate two kinds of quantum phase transitions observed in the one-dimensional half-filled Peierls-Hubbard model with the next-nearest-neighbor hopping integral in the strong-coupling region $U \gg t, t'$ [t (t'), nearest- (next-nearest-) neighbor hopping; U , on-site Coulomb repulsion]. In the uniform case, with the help of the conformal field theory prediction, we numerically determine a phase boundary $t'_c(U/t)$ between the spin-fluid and the dimer states, where a bare coupling of the marginal operator vanishes and the low-energy and long-distance behaviors of the spin part are described by a free-boson model. To exhibit the conformal invariance of the systems on the phase boundary, a multiplet structure of the excitation spectrum of finite-size systems and a value of the central charge are also examined. The critical phenomenological aspect of the spin-Peierls transitions accompanied by the lattice dimerization is then argued for the systems on the phase boundary; the existence of logarithmic corrections to the power-law behaviors of the energy gain and the spin gap (i.e., the Cross-Fisher scaling law) are discussed. [S0163-1829(98)00123-4]

I. INTRODUCTION

Ground states and lower-energy excitations of low-dimensional quantum systems, i.e., a chain, and two- and three-leg ladder materials based on Cu-oxide clusters have attracted great interest in both theoretical and experimental research. In particular, the recently discovered inorganic spin-Peierls (SP) material CuGeO_3 has also intensified interest in the magnetism of one-dimensional (1D) quantum systems coupled to lattice distortion.¹ Although this material is thought to possess non-negligible interchain coupling, it has been confirmed by several experiments that the SP transition occurs at $T_{\text{SP}} \approx 14$ K and the spin gap is estimated as $\Delta \approx 2.11$ meV.¹⁻⁴ Further, doped materials CuZnGeO_3 and CuGeSiO_3 can be synthesized;^{5,6} they enable us to investigate the impurity effects on the spin-gap systems⁷⁻⁹ while it is so far impossible with the organic SP materials.

From structural investigations,¹⁰ it was clarified that the crystal of CuGeO_3 possesses a primitive orthorhombic cell: there are two CuO_6 octahedra sharing a corner and each belongs to a different edge-sharing CuO_2 chain along the c axis, where Ge plays a role of spacer for these chains. As commonly observed in the edge-sharing CuO_2 chain materials (e.g., chains in $\text{Sr}_{14}\text{Cu}_{24}\text{O}_{41}$), since the $2p$ orbitals of oxides cannot be directed towards the nearest-neighbor Cu^{2+} ions, a value of the nearest-neighbor (NN) exchange coupling J is much smaller than those for corner-sharing Cu-oxide materials. Experimentally, J was estimated as 183 K for CuGeO_3 ,¹¹ while, for example, $J \approx 2200$ K for Sr_2CuO_3 .¹² In this situation, it is plausible that the electron hopping processes between next-nearest-neighbor (NNN) Cu^{2+} ions along the Cu-O-O-Cu path become important;¹³ CuGeO_3 may be thus an example of the 1D interacting electron systems with a NNN hopping integral where frustration

effects caused by the hopping process should be strongly reflected in their physical quantities.

As Hase *et al.* reported in their paper,¹ the temperature dependence of the uniform magnetic susceptibility $\chi(T)$ at $T > T_{\text{SP}}$ deviates considerably from the Bonner-Fisher curve, i.e., the theoretical $\chi(T)$ data for the $S = \frac{1}{2}$ antiferromagnetic (AF) Heisenberg spin chain.¹⁴ After that, the Heisenberg spin chain system with the NNN AF exchange couplings ($\gamma J > 0$),

$$H_{J\gamma} = J \sum_l (\mathbf{S}_l \cdot \mathbf{S}_{l+1} + \gamma \mathbf{S}_l \cdot \mathbf{S}_{l+2}), \quad (1)$$

has been used to explain this anomalous behavior: Riera and Dobry¹⁵ obtained $\gamma \approx 0.36$, while Castilla *et al.*¹⁶ estimated $\gamma \approx 0.24$. In both cases, the NNN exchange coupling is estimated to be quite strong, while it is not precisely determined yet. On the other hand, in the case of the inorganic SP material NaV_2O_5 recently discovered by Isobe and Ueda,¹⁷ VO_5 pyramidal clusters share the corners and the magnetic ions $\text{V}^{4+}(3d^1)$ form a chain along the b axis. The experimental data on $\chi(T)$ then agree very well with the Bonner-Fisher curve with $J \approx 560$ K at $T > T_{\text{SP}} \approx 34$ K. This indicates an absence of the NNN exchange coupling and simultaneously presents a behavior that is in sharp contrast to the above-mentioned edge-sharing CuO_2 chain system.

In this paper, we investigate the properties of the edge-sharing Cu-oxide SP system such as CuGeO_3 . More precisely, we shall study effects of the NNN electron hopping process on the ground state and lower-energy excitations, and then clarify the critical phenomenological aspect of the SP transition accompanied by the lattice distortions. As previously discussed by several authors,^{9,18} the 1D half-filled Peierls-Hubbard model may provide a proper framework for

investigating the inorganic SP system. In the present case, however, we should also take the NNN hopping term into account and treat the following Hamiltonian:

$$\begin{aligned}
H = & -t \sum_{\langle l,m \rangle \sigma} [1 + \lambda(u_l - u_m)] (c_{l\sigma}^\dagger c_{m\sigma} + \text{H.c.}) \\
& -t' \sum_{[l,m] \sigma} (c_{l\sigma}^\dagger c_{m\sigma} + \text{H.c.}) + U \sum_l n_{l+} n_{l-} \\
& + \frac{\kappa}{2} \sum_{\langle l,m \rangle} (u_l - u_m)^2, \quad (2)
\end{aligned}$$

where $n_{l\sigma} = c_{l\sigma}^\dagger c_{l\sigma}$ ($\sigma = \pm$). The parameter κ is an elastic constant of the 1D lattice and a displacement of l th Cu^{2+} ion along the c axis (u_l) is coupled to the tight-binding electrons' NN hopping term with strength λ . The summation in the second term runs over all NNN-site pairs $[l,m]$, and this term denotes the NNN hopping process (hereafter we call this term t'). Two electrons with opposite spins feel a repulsive Coulomb interaction $U > 0$ on the same sites. Here, it should be noted that the system with a negative t' value is related to that with $|t'|$ through the particle-hole transformation [i.e., $c_{l\sigma}^\dagger \rightarrow (-1)^l c_{l\sigma}$] in the half-filling case. Therefore, we restrict t' to a positive value in the following discussion.

This paper is organized as follows. In Sec. II, we first investigate the ground-state phase diagram of the system without lattice distortions: The so-called fluid-dimer transition driven by frustration effects is examined in the large- U region. Then the phase boundary is precisely determined in the 2D t' - U parameter space. For the Heisenberg spin chain system, Eq. (1), Okamoto and Nomura obtained the fluid-dimer transition point $\gamma_c \approx 0.2411$ by the use of a numerical method, where the bare coupling of the backward scattering process becomes zero; the low-energy and the long-distance behaviors are then described by the free-boson model (Gaussian model).¹⁹ As we will show in subsequent sections, the spin degrees of freedom of the systems are also described by the free boson on the phase boundary. We shall then numerically check this conclusion according to the conformal field theory (CFT) predictions by Affleck *et al.* (i.e., a value of the central charge and a multiplet structure of excitation spectrum observed in finite-size systems).²⁰ In Sec. III, we discuss the SP instability of the system defined by Eq. (2). The so-called Cross-Fisher scaling law is expected in the same way as the bond alternating $S = \frac{1}{2}$ AF Heisenberg spin chain case.^{21,22} We shall examine this prediction numerically for the systems on the phase boundary; logarithmic corrections to the power-law behaviors will be discussed there, and then results will be compared with those for the $t' = 0$ case, i.e., the 1D half-filled Peierls-Hubbard model. Some discussions are given in Sec. IV, where the correspondence to the results in the weak-coupling region obtained by Fabrizio is discussed.²³ Some relevance to CuGeO_3 is also referred to in this section. Section V is devoted to the short summary of the present investigation.

II. FLUID-DIMER TRANSITION

A. Perturbative treatment in large- U region

In this subsection, in order to investigate the frustration effects caused by the t' term, we perform the

$1/U$ -perturbation expansion²⁴ of Eq. (2) and clarify the spin-gap formation mechanism. Suppose that the lattice dimerization $u_l = (-1)^l u$ and put $\delta = 2\lambda u$. Then up to the third-order perturbation expansion, the effective spin Hamiltonian is given by

$$H_{J\gamma\delta} = J \sum_l \{ [1 + (-1)^l \delta] \mathbf{S}_l \cdot \mathbf{S}_{l+1} + \gamma \mathbf{S}_l \cdot \mathbf{S}_{l+2} \}, \quad (3)$$

where

$$J = \frac{4}{U} \left(1 - 2 \frac{t'}{U} \right), \quad \gamma J = \frac{4}{U} \left(t'^2 - \frac{t'}{U} \right) \quad (4)$$

(hereafter, we take t as an energy unit). Notice that the third-order hopping process along the ‘‘triangle’’ closed loops brings about ferromagnetic couplings. When $u = 0$ (uniform case), the system is reduced to Eq. (1), where the ground-state properties have been closely investigated. Here we briefly summarize the results. Haldane transformed the spin Hamiltonian to a continuous field model and discussed the phase diagram of the ground state.²⁵ Then, using the bosonization technique,²⁶ Kuboki and Fukuyama expressed Haldane's effective model²⁷ by the phase Hamiltonian (quantum sine-Gordon model):

$$\begin{aligned}
\mathcal{H}_{J\gamma} = & \int dx \frac{v_\sigma}{2} \left(2\pi K_\sigma \Pi_\sigma^2 + \frac{1}{2\pi K_\sigma} (\partial_x \Psi_\sigma)^2 \right) \\
& + \int dx D \cos 2\Psi_\sigma, \quad (5)
\end{aligned}$$

where Ψ_σ is the phase variable of the spin degrees of freedom and Π_σ is its canonical conjugate momentum: $[\Psi_\sigma(x), \Pi_\sigma(y)] = i\delta(x-y)$. K_σ and v_σ are the Gaussian coupling and the velocity of the spin excitation, respectively. According to the bosonization procedure, the backward scattering amplitude is approximately given by $D \approx [2aJ/(2\pi\alpha_0)^2](1-3\gamma)$, where the parameters a and α_0 are the lattice constant and a short-distance cutoff, respectively. Following Haldane's argument,²⁵ due to the $\text{SU}(2)$ symmetry of the model in the spin space, the bare coupling constants (K_σ, D) for the spin-fluid state should be located on the so-called Berezinskii-Kosterlitz-Thouless (BKT) line²⁸ embedded in the renormalization-group equations for the quantum sine-Gordon model.²⁹ Then it is apparent that there are only two fixed points: one is the multicritical fixed point $(K_\sigma^*, D^*) = (1, 0)$, which governs systems with $\gamma \leq \gamma_c$ (spin-fluid region) and the other is the strong-coupling fixed point $D^* \rightarrow -\infty$ for $\gamma_c < \gamma$ (dimer region). The fluid-dimer transition point γ_c is thus realized such that the bare amplitude D vanishes. In other words, at this point, logarithmic corrections to physical quantities caused by the marginally irrelevant D term in the spin-fluid region disappear, and the system may be represented by the free-boson model with conformal invariance. On the other hand, in the dimer region $D < 0$, the backward scattering process becomes attractive and the spin excitation acquires a gap described by the same function as the charge gap in the 1D half-filled Hubbard model (i.e., an essential singular form).³⁰

One might expect that the transition point can be numerically determined from the spin-gap data. However, because

of its essentially singular behavior near the transition point, it is difficult to judge whether the gap opens or not. Further, the numerical data may be smeared by the logarithmic corrections. In this situation, a good estimator to determine the transition point may not be spin-gap data but “a multiplet structure” of the excitation spectrum of finite-size systems as discussed in detail by Okamoto and Nomura.¹⁹ They actually evaluated a crossing point of the singlet-singlet and the singlet-triplet excitation gaps for finite-size systems: $\Delta_{ss}(N, \gamma_c(N)) = \Delta_{st}(N, \gamma_c(N))$, equivalently, a point where a fourfold degenerate first excited level is realized. Here,

$$\Delta_{ss}(N, \gamma) \equiv E_1(N, \gamma; 0) - E_0(N, \gamma; 0), \quad (6)$$

$$\Delta_{st}(N, \gamma) \equiv E_0(N, \gamma; 1) - E_0(N, \gamma; 0), \quad (7)$$

and $E_n(N, \gamma; S)$ is an n th excited-state energy of the N -site system in the subspace indexed by the total spin S . Then by extrapolating the data of the finite-size systems, they concluded that $\gamma_c \equiv \gamma_c(\infty) = 0.2411 \pm 0.0001$.

Turning to our electron system, we can approximately predict the fluid-dimer transition line $t'_c(U)$ by the use of both γ_c and Eq. (4): It is given as a solution of the equation

$$0.2411 = \left(t'_c{}^2 - \frac{t'_c}{U} \right) / \left(1 - 2 \frac{t'_c}{U} \right) \quad (8)$$

in the large- U region. In the next subsection, we numerically treat the lattice-fermion systems and evaluate the fluid-dimer phase boundary.

B. Fluid-dimer transition line

Now, we summarize the numerical calculation results on the phase transition line $t'_c(U)$ of the 1D half-filled electron systems [the elastic term in Eq. (2) is ignored in the numerical calculations]. We hereafter suppose that the on-site Coulomb interaction U is sufficiently large so that the charge excitations always acquire a gap due to the umklapp process. In this parameter region, the frustration effects caused by the t' term should bring about the spin gap in accordance with the above scenario; we thus expect that the phase boundary can be accurately determined from the crossing points $t'_c(N, U)$ of the singlet-singlet [$\Delta_{ss}(N, t')$] and singlet-triplet [$\Delta_{st}(N, t')$] excitation gaps of the finite-size systems (we use the same notation for the gaps and the energy levels as in the spin-system case replacing γ with t').

Up to $N=16$ sites, systems were diagonalized by the use of the Lanczos method in the subspaces indexed by quantum numbers, i.e., the total S^z and the total momentum. Figure 1 shows examples of U and t' dependences of Δ_{ss} and Δ_{st} for the 16-site system. The ground state is always singlet. On the other hand, the first excited state is triplet in the spin-fluid region $t' < t'_c(N, U)$, while it is replaced by a singlet state with momentum π (relative to the ground-state value) in the dimer region. According to the Lieb-Schultz-Mattis theorem³¹ for half-integer-spin systems with the translational and the rotational symmetry, the ground state in the dimer region should be degenerate corresponding to the spontaneous broken parity. The first singlet excited state is thus expected to merge to the ground state in the dimer region as $N \rightarrow \infty$. When U is sufficiently large, we observe that Δ_{ss}

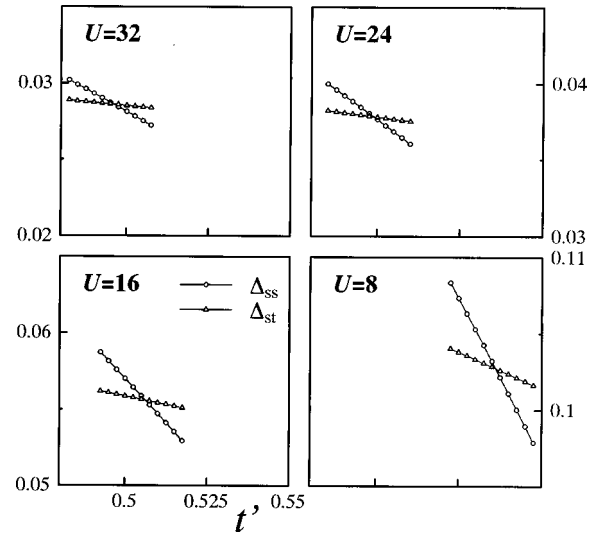


FIG. 1. Singlet-singlet gap $\Delta_{ss}(N, t')$ (circles) and singlet-triplet gap $\Delta_{st}(N, t')$ (triangles) for the 16-site system. The data of $U=8, 16, 24,$ and 32 cases are presented as examples.

becomes zero around $t' \approx \sqrt{1/2}$; this point may be naturally related to the Majumdar-Ghosh model [i.e., Eq. (1) with $\gamma = \frac{1}{2}$] possessing two kinds of NN-singlet array ground states.³²

Performing an interpolation of the diagonalization data, we estimated $t'_c(N, U)$ as shown in Table I. Then, for the $N \rightarrow \infty$ extrapolation, three different algorithms, i.e., Shank’s transform, Wynn’s ϵ algorithm, and the least-square-fitting method assuming the $1/N^2$ dependence of $t'_c(N, U)$ were tried.^{19,33} Results obtained by these different methods are compared, and then we can observe the following: When $U \geq 12$, the consistency among these results holds within 0.2% accuracy, while it becomes worse with the decrease of U , namely, 1% and 5% at $U=8$ and 4 , respectively. Although it may present rough estimation on errors of extrapolated data, the discrepancy is mainly due to a sensitivity of the least-square-fitting method to a staggered N dependence of data. As a consequence, we employ the results of Shank’s transform (Wynn’s ϵ algorithm gives almost the same data). The extrapolation procedure is summarized in Table I (the data of the six-site system were not used).

Figure 2 shows the ground-state phase diagram of the 1D Hubbard model with the NNN transfer integral in the large- U region. Double circles show the extrapolated data in Table I. The broken line exhibits the perturbation result on $t'_c(U)$, i.e., the solution of Eq. (8). The vertical arrow near the x axis denotes the limiting value — $t'_c(\infty) \approx \sqrt{0.2411}$ — expected from the above-mentioned quantum spin case. We can see that calculated data asymptotically converge to the limiting value with the increase of U while the spin-fluid region becomes large in the intermediate- and the weak-coupling regions qualitatively in accordance with the perturbation result; this may be recognized as an itinerancy effect of electrons.

C. Numerical evidence of the conformal invariance

In the spin-fluid region, an effective continuous field model to describe the low-energy excitations of the 1D

TABLE I. The values of $t'_c(N, U)$ (t'_c column) and the extrapolation procedure. The $t'_c{}^{(1)}$ and $t'_c{}^{(2)}$ columns show the data obtained by the iterative application of the Shank transformation.

N	U	t'_c	$t'_c{}^{(1)}$	$t'_c{}^{(2)}$	U	t'_c	$t'_c{}^{(1)}$	$t'_c{}^{(2)}$
6	32	0.506 389 09			16	0.524 614 49		
8		0.499 538 64				0.508 023 33		
10		0.498 009 83	0.495 395 02			0.507 915 19	0.508 037 65	
12		0.497 045 08	0.495 553 33	0.495 458 88		0.506 990 85	0.505 980 59	0.504 313 97
14		0.496 459 22	0.495 350 94			0.506 508 16	0.505 498 90	
16		0.496 075 96				0.506 181 63		
6	28	0.508 312 90			12	0.542 104 48		
8		0.500 489 68				0.515 073 38		
10		0.499 069 47	0.496 181 03			0.517 191 83	0.516 455 06	
12		0.498 117 39	0.496 661 78	0.496 498 69		0.516 062 17	0.515 566 55	0.515 970 85
14		0.497 541 79	0.496 450 74			0.515 717 69	0.514 073 38	
16		0.497 164 98				0.515 432 88		
6	24	0.511 248 06			8	0.585 187 38		
8		0.501 915 34				0.527 89 519		
10		0.500 679 26	0.496 824 89			0.539 438 55	0.536 757 52	
12		0.499 743 33	0.498 350 23	0.498 111 55		0.535 946 45	0.536 447 35	0.536 264 74
14		0.499 183 51	0.498 115 04			0.536 531 23	0.536 298 18	
16		0.498 816 16				0.536 143 77		
6	20	0.516 039 27			4	0.716 713 84		
8		0.504 176 95				0.524 853 17		
10		0.503 290 01	0.528 771 03			0.601 579 21	0.571 281 99	
12		0.502 371 09	0.501 098 89	0.500 705 53		0.551 511 49	0.569 084 44	0.566 737 23
14		0.501 837 55	0.500 801 66			0.578 587 78	0.567 871 12	
16		0.501 485 39				0.560 850 99		

lattice-fermion systems is the free boson with conformal invariance [the so-called $k=1$ SU(2) Wess-Zumino-Witten model]. Affleck, Gepner, Schulz, and Ziman²⁰ discussed the finite-size effects on it and the logarithmic corrections, and further, Nomura and Okamoto³⁴ extended the argument to include the anisotropic quantum spin systems. Some numerical calculation data on the quantum spin systems were also presented there. In this subsection, we shall check the conformal invariance of the interacting lattice fermions: The multiplet structure of the finite-size systems is explored and the value of the central charge is estimated. In general, when we work with the data of the finite-size systems (in the present case, $N \approx 16$ may be the maximum size accessible by the diagonalization method), the logarithmic corrections make these checks difficult. However, as we shall soon show, it is possible for the systems on the phase boundary where the logarithmic correction due to the D term is absent.³⁵

First, three sampling points, i.e., $t'_c(26) = 0.4972$, $t'_c(18) = 0.5017$, and $t'_c(10) = 0.5249$ were picked up from the phase boundary drawn by the spline fitting interpolation of the calculated data (dotted line in Fig. 2). The velocity of spin excitation $v_\sigma(t'_c(U))$ is then extracted from the size dependence of the excitation gap using the relation

$$\frac{2\pi v_\sigma(t'_c)}{N} x_1 \approx \frac{1}{4} [\Delta_{ss}(N, t'_c) + 3\Delta_{st}(N, t'_c)], \quad (9)$$

where x_1 (scaling dimension of the lowest excitations) is assumed to $\frac{1}{2}$.^{19,36} Since the linearity of the data is excellent (see Fig. 3), we can estimate $v_\sigma(t'_c)$ accurately using the least-square-fitting method for the data (except for those of the six- and eight-site systems).

Next we evaluate the central charge c : The ground-state energy of the system with the periodic boundary condition is given by

$$E_0(N, t'_c; 0) \approx e_0 N - \frac{\pi v_\sigma(t'_c)}{6N} c, \quad (10)$$

where e_0 is the ground-state energy density in the thermodynamic limit. Figure 4 shows the $1/N^2$ dependence of E_0/N at the sampling points. The least-square-fitting lines show $c \approx 1$ within 4% independently of the points. As a result, we can conclude that since the $t'_c(U)$ dependence is only reflected in the velocity of excitation, the systems on the phase boundary are identical to the free-boson model, and thus, its criticality is described by the $c=1$ CFT.

Finally, we investigate multiplet structures of finite-size systems on the phase boundary. The lower-energy excitation levels are measured with taking the ground-state energy as zero and normalized by the velocity as^{20,37}

$$x \equiv [E_n(N, t'_c; S) - E_0(N, t'_c; 0)] / \frac{2\pi v_\sigma(t'_c)}{N}. \quad (11)$$

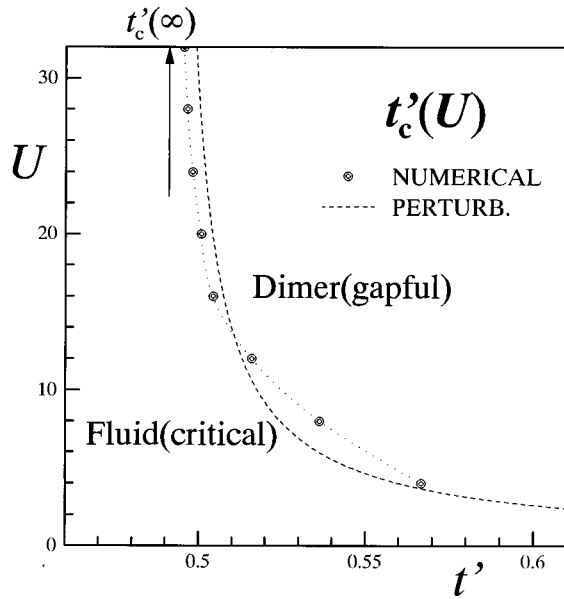


FIG. 2. Ground-state phase diagram of the 1D half-filled Hubbard model with the NNN transfer integral. The double circles denote the extrapolated data of the transition point and the broken line is the perturbatively estimated phase boundary. The arrow near the x axis shows the value for the frustrated Heisenberg spin chain system [$t'_c(\infty) \approx \sqrt{0.2411}$].

Results are then summarized in Fig. 5. When N is small, the numerical data considerably deviate from the CFT prediction (dotted lines in the figure). This may be mainly due to the $O(1/N^3)$ corrections from the irrelevant operators that are dropped when we take the continuous limit of the lattice model. On the other hand, with the increase of N , we can find that the supermultiplet structure becomes prominent independently of the sampling points and the data clearly reproduce the high degeneracy of the CFT prediction.

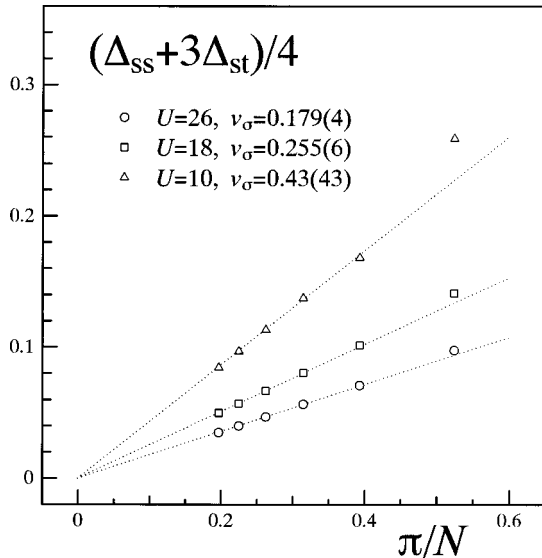


FIG. 3. The system size dependence of the averaged excitation gap at the sampling points. The velocity of the spin excitation (v_σ) is extracted from the least-square-fitting lines (dotted lines). The parenthesized digits in the figure include errors.

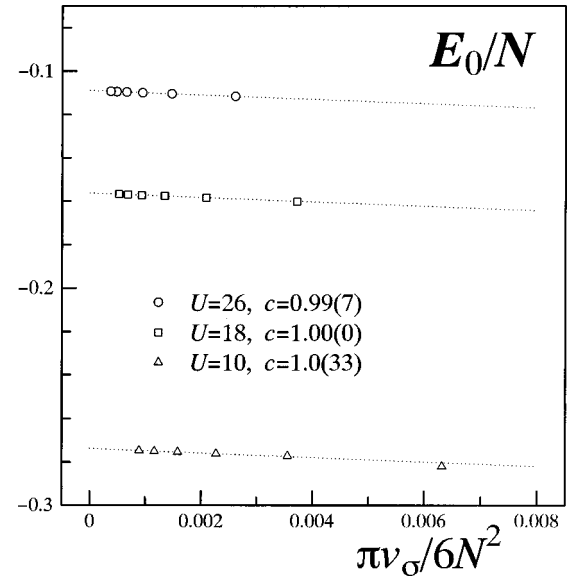


FIG. 4. The system size dependence of the ground-state energy density at the sampling points. The value of the central charge (c) is estimated from the gradient of least-square-fitting lines (dotted lines). The parenthesized digits in the figure include errors.

III. SPIN-PEIERLS TRANSITION

A. Cross-Fisher scaling law

So far, we have investigated the uniform case and discussed the frustration effects on the spin-fluid state. Now, we shall discuss another gap formation mechanism embedded in Eq. (2), i.e., the SP instability. In the large- U region, we can start with the effective Hamiltonian Eq. (3) with assuming the lattice dimerization. Then its bosonized form is well known; i.e., a nonlinear term (we call this the B term) emerging from the bond alternation,

$$\mathcal{H}_u = \int dx B \cos \Psi_\sigma \quad (12)$$

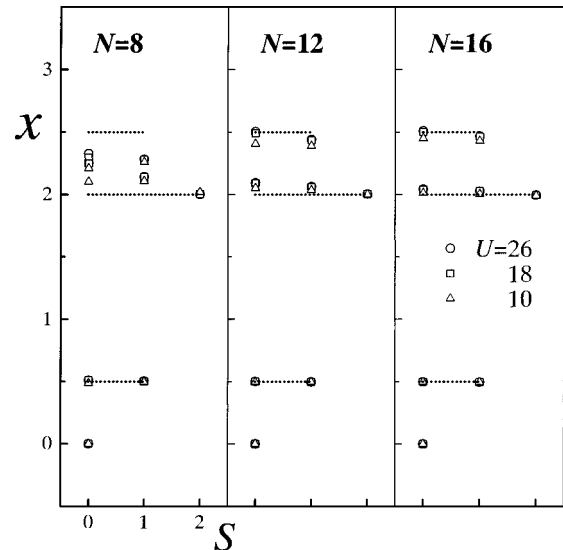


FIG. 5. Examples of system size dependence of the lower-energy excitation levels (normalized). Triangles, squares, and circles denote the data at $t'_c(10)$, $t'_c(18)$, and $t'_c(26)$, respectively. Dotted lines show the CFT prediction.

($B \propto u$), is appended to Eq. (5). As mentioned above, since the D term is marginally irrelevant in the spin-liquid region, the couplings are renormalized to $(K, D) \rightarrow (1, 0)$. On the other hand, the B term becomes relevant and leads to a critical phenomena (critical point $u_c = 0$), where the power-law behaviors of two physical quantities, i.e., the ground-state energy gain due to the lattice dimerization (per site) $G(u) \propto u^{2-\alpha}$ and the singlet-triplet excitation gap $\bar{\Delta}_{\text{st}}(u) \propto u^\nu$ are the main concerns: According to Cross and Fisher, these critical exponents are given as

$$(\alpha, \nu) = \left(\frac{2}{3}, \frac{2}{3} \right), \quad (13)$$

respectively (Cross-Fisher scaling law²¹) and further, they satisfy the hyperscaling relation of exponents $d\nu = 2 - \alpha$ ($d = 1 + 1$). However, in general, it is naturally expected that the power-law behaviors acquire logarithmic corrections in the course of the renormalization of the marginally irrelevant operator.³⁸ In fact, in the previous paper, we have numerically studied the $t' = 0$ case assuming the uniform charge distribution (i.e., the absence of a ‘‘charge soliton’’).¹⁸ The results show that the Cross-Fisher scaling law acquires the logarithmic corrections, e.g., $\bar{\Delta}_{\text{st}}(u) \propto u^{2/3}/|\ln u|$. In the present case ($t' \neq 0$), however, as we have seen in Sec. II, the main effect of the t' term in the large- U region is to introduce the frustration; the bare coupling of the D term decreases with the increase of t' , and finally, it vanishes at $t' = t'_c(U)$. Therefore, we expect that since logarithmic corrections may be absent from the SP transition of the systems on the fluid-dimer transition line, the critical behavior is clearly visible even for working with small-size systems.

B. Numerical results

In this subsection, we summarize the numerical data on the lattice-dimerization effects [$u_l = (-1)^l u$]. The diagonalization calculations were performed for the systems on the above-mentioned sampling points. Systems of up to 16 sites were treated and the following parameter values were used for the evaluation of critical exponents: $\lambda = 1$ and $u = e^{-\rho}$ ($\rho = 1, 2, \dots, 11$) (in unit of t). Suppose that $\bar{E}_0(N, u; S)$ is the ground-state energy of the N -site system in the subspace of the total spin S . Then, the energy gain per site and the singlet-triplet gap are defined by

$$N\bar{G}(N, u) \equiv \bar{E}_0(N, 0; 0) - \bar{E}_0(N, u; 0), \quad (14)$$

$$\bar{\Delta}(N, u) \equiv \bar{E}_0(N, u; 1) - \bar{E}_0(N, u; 0), \quad (15)$$

respectively (physical quantities with the bar denote the data on the phase boundary).

First, according to the finite-size scaling hypothesis, the numerical data are analyzed with assuming the one-parameter scaling form

$$Q(N, u) \sim N^{-\mu_Q} f_Q(N/\xi) \sim N^{-\mu_Q} f_Q(Nu^\nu), \quad (16)$$

where $Q = \bar{G}$ or $\bar{\Delta}$. ξ is the correlation length (inverse of the spin gap) and f_Q is an universal scaling function. From the limiting behaviors, i.e., $\bar{G}(\infty, u) \sim u^{2-\alpha}$, $\bar{G}(N, u) \sim u^2$ with

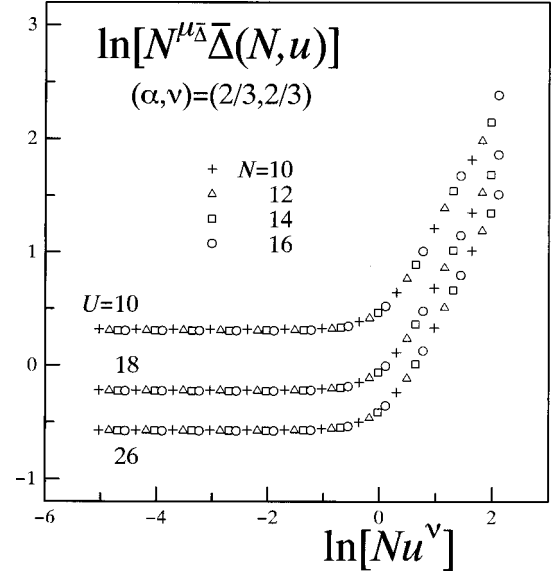


FIG. 6. Finite-size scaling plot of the singlet-triplet excitation gap at the sampling points. The Cross-Fisher exponents are used for plots of $\ln[N^{\mu_{\bar{\Delta}}}\bar{\Delta}(N, u)]$ vs $\ln(Nu^\nu)$.

fixed N (Ref. 39) and $\bar{\Delta}(\infty, u) \sim u^\nu$, $\bar{\Delta}(N, 0) \sim 1/N$,⁴⁰ the exponents μ_Q and the asymptotic behaviors of f_Q are expected as follows: $\mu_{\bar{G}} = (2 - \alpha)/\nu$,

$$f_{\bar{G}}(x) \rightarrow \begin{cases} x^{2/\nu} & \text{for } x \rightarrow 0 \\ x^{(2-\alpha)/\nu} & \text{for } x \rightarrow \infty, \end{cases} \quad (17)$$

and $\mu_{\bar{\Delta}} = 1$,

$$f_{\bar{\Delta}}(x) \rightarrow \begin{cases} \text{const} & \text{for } x \rightarrow 0 \\ x & \text{for } x \rightarrow \infty. \end{cases} \quad (18)$$

In general, α and ν are fitting parameters to be determined from the scaling plots. However, if we employ the Cross-Fisher exponents and these asymptotic behaviors, no adjustable parameter exists in the finite-size scaling analysis.

Figures 6 and 7 show the plots of the spin gap and the energy gain per site with $(\alpha, \nu) = (\frac{2}{3}, \frac{2}{3})$, respectively (the data of $N = 10, 12, 14$, and 16 cases were used). The curves in Fig. 7 have been shifted appropriately along the y axis for clarity. We can see from these figures that in spite of working with small-size systems the scaled data collapse on universal functions within good accuracy and their asymptotic behaviors agree with expected ones in both figures. Further, these scaling properties do not depend upon the sampling points as we have expected. Therefore, the present numerical data analysis seems to indicate that the SP transition of the systems on the phase boundary is in accord with the Cross-Fisher scaling law.

Here, it should be noted that Chitra *et al.*⁴¹ studied the $S = \frac{1}{2}$ Heisenberg spin chain, Eq. (3), at $\gamma = \gamma_c$ by the use of the density-matrix renormalization-group (DMRG) method.⁴² They obtained critical exponents $(\alpha, \nu) \approx (0.749, 0.667)$, which indicate violation of the hyperscaling relation of exponents in the SP transition. On the other hand, Okamoto and Nakamura⁴³ recently reexamined the same problem using the exact diagonalization method; the spin gap and the

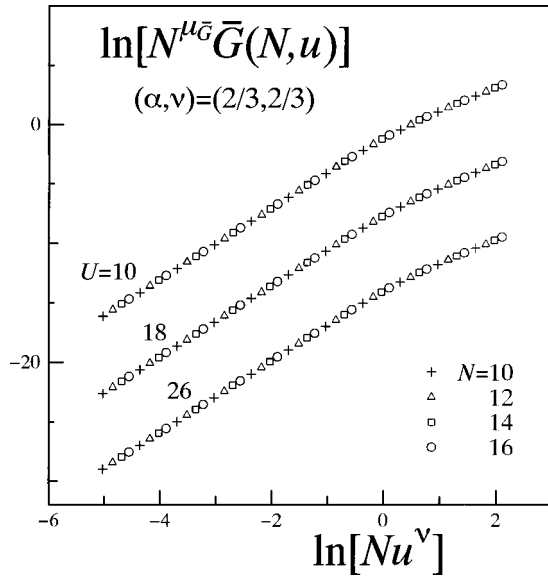


FIG. 7. Finite-size scaling plot of the energy gain per site at the sampling points. The Cross-Fisher exponents are used for plots of $\ln[N^{\mu_{\bar{G}}}\bar{G}(N,u)]$ vs $\ln(Nu^{\nu})$. The curves have been shifted along the y axis for clarity (0, -6, and -12 for $U=10, 18$, and 26 , respectively).

energy gain data were analyzed according to the finite-size scaling hypothesis. In particular, the possibility of a logarithmic correction to the energy gain,

$$\bar{G} \propto \delta^a |\ln \delta|, \quad (19)$$

was discussed in detail there. As a result, they concluded that the SP transition at $\gamma = \gamma_c$ is described by the Cross-Fisher scaling law except for the existence of the logarithmic correction to the energy gain, i.e., by Eq. (19) with $a = \frac{4}{3}$.

In order to investigate this possibility in our case, we employ a cost function S_{LLF} (local linearity function) to measure the universal fitting of scaling plots as explained below.⁴⁴ Suppose that (x_i, y_i) [$i = 1, \dots, n$, $(x_i < x_{i+1})$] are a scaled variable and a scaled physical quantity, respectively [$x_i = \ln(Nu^{\nu})$ and $y_i = \ln(N^{\mu_{\bar{G}}}\bar{G})$ in our data analysis]. Then the quantity

$$S_{\text{LLF}} = \sum_{i=2}^{n-1} \left(\frac{y_i - \langle y_i \rangle}{d_i} \right)^2 \quad (20)$$

gives a local linearity of a function and may serve to measure the reliability of the universality of scaling plots, where $\langle y_i \rangle = [(x_{i+1} - x_i)y_{i-1} - (x_{i-1} - x_i)y_{i+1}] / (x_{i+1} - x_{i-1})$ and $d_i^2 = 1 + [(x_{i+1} - x_i)^2 + (x_{i-1} - x_i)^2] / (x_{i+1} - x_{i-1})^2$. We fixed $\nu = \frac{2}{3}$ and calculated S_{LLF} as a function of $\mu_{\bar{G}}$; the obtained results are summarized in Fig. 8. The implications of the observed behaviors are rather subtle and there may be two possibilities: We find that the optimized values $\mu_{\bar{G}}^*$ are always smaller than 2 (the Cross-Fisher case) independently of the sampling point while a staggered size dependence is visible at $U = 10$. This tendency seems to coincide with the frustrated Heisenberg spin system case as mentioned above, and thus the deviation from $\mu_{\bar{G}}^* = 2$ might be attributed to the logarithmic correction, Eq. (19). On the other hand, it is also

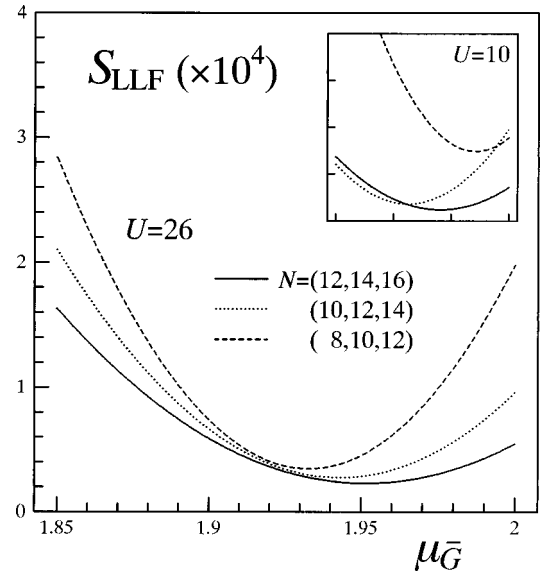


FIG. 8. The $\mu_{\bar{G}}$ dependence of the local linearity function S_{LLF} with $\nu = \frac{2}{3}$. The solid, the dotted, and the broken lines show the results obtained from $N=(12,14,16)$, $(10,12,14)$, and $(8,10,12)$ sites systems' data, respectively. The inset shows the results at $U=10$.

plausible that since $\mu_{\bar{G}}^* \approx 1.95$ is enough close to 2, the deviation does not have to indicate the existence of the logarithmic correction but other artificial effects in the present data analysis (e.g., a parameter range to be examined or unexpected features of the cost function). As a result, we could not detect the existence of the logarithmic correction claimed in the quantum spin system case; more intensive investigations should be conducted to draw a definitive conclusion by the use of other numerical approaches.

IV. DISCUSSIONS

In our investigation at half-filling, we have assumed that the system is in the insulating phase due to the relevant umklapp process in the large- U region (i.e., in the single-component Tomonaga-Luttinger liquid state). On the other hand, recently, Fabrizio explored the ground-state phase diagram of the 1D Hubbard model with the t' term.²³ Since their approach is based on both the bosonization starting from the noninteracting fermion system and the perturbative renormalization-group calculations, the predictions may hold in the weak-coupling region, and thus it is complimentary to our investigation. In the half-filling case, significant effects of the t' term are observed in $t' > 0.5$ region, where four Fermi points exist, and thus the two-band effective model can describe the low-energy excitation properties. In this situation, the scaling dimension of the umklapp process becomes higher since four electrons at the Fermi points commensurately participate in the scattering process. As a consequence, the umklapp process is not always relevant; the charge excitation, in turn, possibly becomes gapless below a certain critical value U_c . This possibility was numerically investigated by Kuroki *et al.*⁴⁵ with employing the DMRG method. Consequently they estimated $U_c(t'=0.8) \approx 3$, although the determination of the critical value as an end point of the massless phase may be difficult.

According to the prediction by Fabrizio, at half-filling, the magnetic insulating (MI) and the dimer insulating (DI) phases are realized when U is large. On the other hand, the superconducting (SC) region is expected in the small- U region, where the charge (spin) gap is closed (open). In fact, the MI and the DI phases are identical with the spin-liquid and the dimer states in the present investigation, but the SC region is apparently beyond the scope of our discussion. Therefore, to complete the phase diagram in the 2D t' - U parameter space, we should also examine the charge excitations in the weak-coupling region (e.g., t' dependence of U_c) and clarify the transition properties between expected phases.

We have treated the 1D fermion system and clarified its basic properties, i.e., ground-state phase diagrams and the criticality of the SP transition. However, it is known for the real inorganic compound CuGeO_3 that interchain coupling is quite strong [i.e., J_b (exchange coupling constant along the b axis) $\sim 0.1J$].³ Inagaki and Fukuyama⁴⁶ discussed the phase boundary between the Néel and the SP states by taking the interchain coupling into account (within the scope of the mean-field approximation), and quite recently Zang *et al.* extended the argument to include the frustration.⁴⁷ The results indicate that the frustration, relatively speaking, favors the SP state over the Néel one; therefore that the SP state is observed in CuGeO_3 despite the non-negligible interchain coupling might be due to the strong frustration effect originating from Cu-O-O-Cu electron hopping process. On the other hand, if the system is in the dimer phase in Fig. 2, there are no critical phenomena when the lattice dimerization is taking place, and hence the model can not describe the SP system.⁴ These conditions naturally put CuGeO_3 near the fluid-dimer phase boundary. However, for a quantitative discussion on the values of model parameters, more detailed numerical and analytical investigations including the dynamical and the finite-temperature properties of the present lattice-fermion system should be conducted.^{15,16,48}

V. SUMMARY

In this paper, we have investigated the ground state and the lower-energy excitations of the one-dimensional half-filled Peierls-Hubbard model with the next-nearest-neighbor hopping integral. First the transition between the spin-fluid and the dimer states that is driven by the frustration effect introduced by the next-nearest-neighbor hopping process was discussed in the uniform case; the phase boundary $t'_c(U/t)$ was numerically determined using the level crossing method based on the conformal field theory prediction. Further, for the systems on the phase boundary, we checked the conformal invariance by exploring the multiplet structure of the low-energy excitation spectrum and estimating the value of the central charge.

Next, we discussed the critical phenomenological aspect of the spin-Peierls transition accompanied by the lattice dimerization. The numerical data for the systems on the phase boundary seem to indicate the power-law behaviors of the energy gain and the spin gap in accordance with the prediction by Cross and Fisher. More detailed analysis employing the cost function to measure the universal fitting of the finite-size scaling plots, however, exhibits a small discrepancy between the optimized value and the predicted one on the energy gain exponent. One of the possibilities might be that the deviation is due to the contribution from the logarithmic correction as claimed in the recent investigation on the frustrated Heisenberg spin chain system. Nevertheless, this subject is still controversial in the case of our lattice-fermion system.

ACKNOWLEDGMENTS

The author is grateful to Y. Okabe, T. Nishino, and K. Okamoto for helpful discussions. The main computations were carried out on FACOM VPP550 at the Supercomputer Center, Institute for Solid State Physics, University of Tokyo.

-
- ¹M. Hase *et al.*, Phys. Rev. Lett. **70**, 3651 (1993).
²K. Hirota *et al.*, Phys. Rev. Lett. **73**, 736 (1994).
³M. Nishi *et al.*, Phys. Rev. B **50**, 6508 (1994).
⁴Q. J. Harris *et al.*, Phys. Rev. B **50**, 12 606 (1994).
⁵M. Hase *et al.*, J. Phys. Soc. Jpn. **65**, 1392 (1996).
⁶J. P. Renard *et al.*, Europhys. Lett. **33**, 475 (1995).
⁷L. P. Regnault *et al.*, Europhys. Lett. **32**, 579 (1995).
⁸H. Fukuyama *et al.*, J. Phys. Soc. Jpn. **65**, 1182 (1996).
⁹H. Yoshioka and Y. Suzumura, J. Phys. Soc. Jpn. **66**, 3962 (1997).
¹⁰G. A. Petrakovskii *et al.*, Zh. Éksp. Teor. Fiz. **98**, 1382 (1990) [Sov. Phys. JETP **71**, 772 (1990)].
¹¹H. Nojiri *et al.*, Phys. Rev. B **52**, 12 749 (1995).
¹²N. Motoyama *et al.*, Phys. Rev. Lett. **76**, 3212 (1996).
¹³J. E. Lorenzo *et al.*, Phys. Rev. B **50**, 1278 (1994).
¹⁴J. C. Bonner and M. E. Fisher, Phys. Rev. **135**, A640 (1964).
¹⁵J. Riera and A. Dobry, Phys. Rev. B **51**, 16 098 (1995).
¹⁶G. Castilla *et al.*, Phys. Rev. Lett. **75**, 1823 (1995).
¹⁷M. Isobe and Y. Ueda, J. Phys. Soc. Jpn. **65**, 1178 (1996).
¹⁸H. Otsuka, Phys. Rev. B **56**, 15 609 (1997).
¹⁹K. Okamoto and K. Nomura, Phys. Lett. A **169**, 433 (1992); S. Eggert, Phys. Rev. B **54**, R9612 (1996).
²⁰I. Affleck, D. Gepner, H. J. Schultz, and T. Ziman, J. Phys. A **22**, 511 (1989).
²¹M. C. Cross and D. S. Fisher, Phys. Rev. B **19**, 402 (1979).
²²T. Nakano and H. Fukuyama, J. Phys. Soc. Jpn. **49**, 1679 (1980); *ibid.* **50**, 2489 (1981).
²³M. Fabrizio, Phys. Rev. B **54**, 10 054 (1996).
²⁴M. Takahashi, J. Phys. C **10**, 1289 (1977).
²⁵F. D. M. Haldane, Phys. Rev. B **25**, 4925 (1982); **26**, 5257 (1982).
²⁶For review, V. J. Emery, in *Highly Conducting One-Dimensional Solids*, edited by J. T. Devreese (Plenum, New York, 1979); H. Fukuyama and H. Takayama, in *Electronic Properties of Inorganic Quasi One-Dimensional Compounds*, edited by P. Monceau (Reidel, New York, 1984).
²⁷K. Kuboki and H. Fukuyama, J. Phys. Soc. Jpn. **56**, 3126 (1987).
²⁸V. L. Berezinskii, Zh. Éksp. Teor. Fiz. **61**, 1144 (1971) [Sov. Phys. JETP **34**, 610 (1972)]; J. M. Kosterlitz and D. J. Thouless, J. Phys. C **6**, 1181 (1973); J. M. Kosterlitz, *ibid.* **7**, 1046 (1974).
²⁹For example, J. B. Kogut, Rev. Mod. Phys. **51**, 659 (1979).
³⁰E. H. Lieb and F. Y. Wu, Phys. Rev. Lett. **20**, 1445 (1968).

- ³¹E. H. Lieb, T. Schultz, and D. J. Mattis, *Ann. Phys. (N.Y.)* **16**, 407 (1961).
- ³²C. K. Majumdar, *J. Phys. C* **3**, 911 (1970); C. K. Majumdar and D. K. Ghosh, *J. Math. Phys.* **10**, 1399 (1969).
- ³³For example, M. N. Barber, in *Phase Transitions and Critical Phenomena*, edited by C. Domb and J. L. Lebowitz (Academic Press, New York, 1983), Vol. 8, p. 145.
- ³⁴K. Nomura and K. Okamoto, *J. Phys. A* **27**, 5773 (1994).
- ³⁵R. Jullien and F. D. M. Haldane, *Bull. Am. Phys. Soc.* **28**, 34 (1983); F. D. M. Haldane, *Phys. Rev. Lett.* **60**, 635 (1988).
- ³⁶T. Giamarchi and H. J. Schulz, *Phys. Rev. B* **39**, 4620 (1989).
- ³⁷J. L. Cardy, *J. Phys. A* **17**, L385 (1984).
- ³⁸J. L. Black and V. J. Emery, *Phys. Rev. B* **23**, 429 (1981).
- ³⁹K. Okamoto *et al.*, *J. Phys. Soc. Jpn.* **55**, 1458 (1986); H. Nishimori and K. Okamoto, *ibid.* **56**, 1132 (1987).
- ⁴⁰A. A. Ovchinnikov, *Zh. Éksp. Teor. Fiz.* **57**, 2137 (1969) [*Sov. Phys. JETP* **30**, 1160 (1970)]; M. Takahashi, *Prog. Theor. Phys.* **43**, 1619 (1970).
- ⁴¹R. Chitra *et al.*, *Phys. Rev. B* **52**, 6581 (1995).
- ⁴²S. R. White, *Phys. Rev. Lett.* **69**, 2863 (1992); *Phys. Rev. B* **48**, 10 345 (1993).
- ⁴³K. Okamoto and T. Nakamura, *J. Phys. A* **30**, 6287 (1997).
- ⁴⁴N. Kawashima and N. Ito, *J. Phys. Soc. Jpn.* **62**, 435 (1993).
- ⁴⁵K. Kuroki, R. Arita, and H. Aoki, *J. Phys. Soc. Jpn.* **66**, 3371 (1997).
- ⁴⁶S. Inagaki and H. Fukuyama, *J. Phys. Soc. Jpn.* **52**, 3620 (1983).
- ⁴⁷J. Zang, S. Chakravarty, and A. R. Bishop (unpublished).
- ⁴⁸H. Yokoyama and Y. Saiga *J. Phys. Soc. Jpn.* **66**, 3617 (1997).